PASJ: Publ. Astron. Soc. Japan **999**, 999–5 (2000)

X-Rays from Gamma Cassiopeiae with ASCA

Shin Kubo, Toshio Murakami, Manabu Ishida
The Institute of Space and Astronautical Science,
3-1-1 Yoshinodai, Sagamihara, Kanagawa 229 Japan
E-mails: murakami and skubo@astro.isas.ac.jp
and
Robin H. D. Corbet
Laboratory for High Energy Physics, NASA, GSFC
Greenbelt, MD 20771, USA

(Received 1997 ; accepted 1998)

Abstract

X-rays from γ Cassiopeiae were observed to understand the origin of them with *ASCA*. Since the discovery of X-rays from this system, several possible origins of X-rays have been suggested including the coronal origin of γ Cas itself, the binary neutron star origin and the binary white dwarf origin of them. However there was no firm fact to distinguish these models. The *ASCA* SIS detectors, which are now the best X-ray energy resolving power were used and resolved iron lines on the continuum spectrum. The spectrum with the lines is compared with the well-known X-ray spectra such as the hot corona of early type stars, the low-mass binaries, the high mass binaries and the white dwarf binaries. The observed rapid fluctuation of about 10 s and the spectrum of 10.6 keV in temperature with iron lines prefer this system to be in a binary white dwarf system. Assuming a white dwarf binary for X-ray emitter, we estimate the most probable luminosity of this system based on the recent observed stellar wind data to answer to the lack of luminosity mentioned in the previous papers.

Key words: X-rays: spectra—Stars: individual (γ Cas)

1. Introduction

γ Cassiopeiae is one of the best known Be star, which is the first emission-line star discovered (Angelo Secchi 1866), and is classified into B0IVe (Hoffleit and Warren 1991). This star is long known to be very variable in optical and is also known as the moderately strong X-ray source with the luminosity of order 10^{33} erg s^{-1} (Mason et al. 1976, White et al. 1982). This luminosity is not surprising to be X-rays from early type stars such as O and B types (Chlebowski and Harnden 1989; Corcoran et al. 1994). Some of the active early type stars showed this luminosity range(Corcoran et al. 1994, Koyama et al. 1994). However the hardness of X-rays from γ Cas is extraordinarily high compared with the ordinary X-ray stars from early type stars (Corcoran et al. 1994, Koyama et al. 1994). If we fit the spectrum with a thermal model, the resultant temperature was roughly 10 keV or more (Horaguchi et al. 1994, Murakami et al. 1986). This is not common to early type stars and more resembles to X-ray pulsars and accreting white dwarf binaries. Based on the hard spectrum, some suggest the origin of X-rays from an unseen binary neutron star (Marlborough et al. 1978; Rappaport and Heuvel 1982; White et al. 1982) and some suggest an unseen binary dwarf companion (Murakami et al. 1986, Horaguchi et al. 1994, Haberl 1995). Recently Smith suggested a third possible model to explain the X-rays as the result of hot spots on γ Cas itself (Smith et al. 1998). Although, there are no evidence of a binary nature of this system, a neutron star binary model can easily explain the observed luminosity and the hard spectrum. No observed evidence of binary motion makes the white dwarf model difficult in explaining the moderate luminosity, but the thermal spectrum with the temperature of 10 keV looks suitable for this model. The coronal origin of X-rays also comes from no observed orbital motion of this system and rather active Be star of γ Cas . The most recent hot spots model on the star surface comes from the probable rotation related in X-ray variability (Smith et al. 1998) and the resemblance to late type stars with flare activities like RS-CVns which show high temperature and very variable. What can ASCA say to these different models to explain X-rays from γ Cas ? ASCA has the best energy resolving power than before and good signal to noise ratio. We also recalculate the most probable luminosity in the case of a wind accretion onto the white dwarf star based on the most recent observational data of mass distribution in the wind (Stee et al. 1995).

2. Observation

2.1. ASCA Instruments and Observations

The observations with *ASCA* were done at three independent days on 1996 January 18, March 3 and September 4. In total, 4, 10 and 6 ks were accumulated respectively. *ASCA* carries four telescopes, each with a detector sensitive in the 0.5–10.0 keV range. The spatial resolution of the mirrors is about 3' half power beam width (HPBW). Two mirrors are for solid state imaging spectrometers (SIS) using CCDs, and two are for gas scintillation imaging spectrometers (GIS). The SIS has a high-spectral resolution, about 180 eV full width at half maximum (FWHM) at 6 keV, whereas the GIS has a higher detector efficiency at the upper end of the observing band, but a lower spatial resolution. The GIS has a FOV of 50' diameter, whereas each SIS has a FOV of 11'× 11' in one CCD mode. The observations of γ Cas were carried out using this one CCD mode. The CCDs are read slowly, every 4 s, while in the GIS, depending on the mode, and each photon is time-tagged to a resolution of between 61 μs and several ms. More details concerning the instrumentation on-board the *ASCA* satellite have been reported separately (Tanaka, Inoue, and Holt 1994, Makishima et al. 1996, Serlmitsos et al. 1995, Yamashita et al. 1997). At the planning, we intended to observe γ Cas simultaneously with *RXTE* and *EUVE*, but due to unexpected malfunction of operation of *ASCA*, the first observation was suddenly truncated into small two parts. As the recovery of the malfunction of observation, *ASCA* has observed again on March and September independently with other satellites. So we simply report the *ASCA* observations alone without any connection of other satellite observations.

2.2. Intensity variation in each data

The intensity variations of the three data sets, averaged over four instruments (SIS0, SIS1, GIS2 and GIS3), are shown in figure 1a to figure 1c with a time resolution of 16 s in 2–10 keV after the background subtraction. The intensities look very variable and the doubling time of about 64 s is clear in the figure 1c at 24.1 hour position. The fastest fluctuation recorded during the ASCA observations was about 10 s as shown in the figure 1d at 25.53 hour position. There was no clear hardness change during this rapid fluctuation, so this was not an absorption. This time scale limits the upper most size of the emission region of 3×10^{11} cm. This is much smaller than the size of the Be star γ Cas itself. We have carried out the period searches, which were suggested before (Frontera et al. 1987, Haberl 1995). We could not confirm the 135.6 min period reported before by Haberl (1995). Although we could not find any periodicity between 3.5×10^{-5} Hz to 3×10^{-2} Hz, the 1/f type fluctuation is clear to the data set but the power densities saturate at around 10^{-3} Hz to lower. Figure 2 shows a power density plot by the XRONOS software to the data averaged over figure 1a to 1c together with the 1/f fit.

2.3. Spectrum Analysis

Although the intensity of this source was very variable, the hardness ratios, which represents the spectrum, did not show clear correlation with the intensity. So we added all three data sets into one to have a better signal to noise ratio. Then a spectrum of the X-ray source has been derived with great care. At first, the background must be carefully selected within the same FOV in order to subtract out any possible nearby galactic component. The data from the SIS detector were cleaned of hot and flickering pixels, and selected based on appropriate values of object elevation and magnetic rigidity. However due to the limited background, the standard "blank sky" observation provided by the *ASCA* Guest Observer Facility, is then added and subtracted. A spectrum was extracted from all photons lying within 3' radius circle centered on the source. The derived SIS spectrum is shown in figure 3 together with a fit model. First we have fitted the data using a single power-law. It is clear that there is an excess at around 6.7 keV. Although a power-law with a Gaussian line with a finite line width fits to the data well, however much wider energy coverage of the previous GINGA data clearly excluded the power-law model in explaining the continuum shape (Horaguchi et al. 1994). There was no known X-ray system which showed a single power-law with a strong 6.7 keV iron line. Then we have fitted the data using the Raymond-Smith and/or Meka thermal model as a temperature and the abundance are free. The 10.6 keV in temperature with 0.35 solar model fits to the data in both cases. These models show already acceptable chi-value but the residual looks some systematic at an iron line of 6.4 keV and also at around 1 keV. The artificially added 6.4 keV iron line, Ne at 0.92 keV(He-like) and 1.02 keV(H-like) to the R-S model fit very well as shown in the figure-3c. Table 1 summarizes the best-fit parameters for these models and their $\pm 90\%$ errors. The observed flux in the band 2–10 keV is 1.2×10^{-12}erg s^{-1}cm^{-2}. Assuming the optically thin thermal emission model, we have obtained the bolometric luminosity to be 1.8×10^{33}erg s^{-1} at the distance of 220 pc (Schmidt-Kaler 1964). The 0.35 in abundance is also common to a white dwarf system and the most X-ray stars observed with *ASCA* (Fujimoto and Ishida 1997, Done et al. 1997, Ishida et al. 1997, Kallman et al. 1996, Corcoran et al. 1994, Koyama et al. 1994). The most significant feature of the spectra were its high temperature of almost 10 keV and the iron lines which are consistent with the temperature. The existence of cold iron together with a high temperature plasma is not contradicting. Many X-ray stars with massive binary have shown strong neutral iron line caused by the reflection of cold wind materials. So the existence of cooler neutral component together with the highly ionized iron does not contradict each other.

3. Discussion

X-ray spectra of γ Cas were obtained from the previous X-ray satellites so far in orbit. Among them, *Tenma* and *Ginga* observations (Murakami et al. 1986, Horaguchi et al. 1994) concluded that the observed spectra were fitted significantly better by the thermal bremsstrahlung than by the power-law. The temperatures of the thermal bremsstrahlung were obtained to be 11.7$\pm$0.8 keV and 16.8 $\pm$ 0.1 keV, respectively, by *Tenma* and *Ginga*. On the other hand, *EXOSAT* observation found no difference between the thermal bremsstrahlung model and the power-law model. This is simply understood as the temperature of γ Cas is so high that a detector with no sensitivity above 10 keV cannot distinguish the thermal spectrum from the power-law. From the *ASCA* observation, we found the iron emission lines, whose central energies locate at 6.7 keV and 6.9 keV. These components are expected from the optically thin thermal plasma whose temperature is more than 10 keV. Following *Tenma* and *Ginga*, we stress again that the hard X-rays of γ Cas originate from optically thin thermal plasma with the temperature of $\sim$10 keV.

The thermal spectrum with 10 keV in temperature and at least two highly ionized iron lines and the probable third neutral iron line resemble to the spectra of white dwarf binary systems (Kallman et al. 1996, Fujimoto and Ishida 1997). In this discussion, we list all the known point X-ray systems and compare the observed characteristics of γ Cas with these systems.

First we list single stars. The coronal origin of early type main stars from O and B types are clearly excluded by the rapid fluctuation of about 10 s observed in this observation. The size of corona of early type star is much larger than the size of 10 light-sec. The X-rays from late type stars from G to M with X-ray coronal activities are too short to be the luminosity of 10^{33} erg sec^{-1}. More over, all X-ray temperatures above are significantly below 3 keV and not reached to 10 keV of γ Cas including the late type stars. We do not know any example of X-rays from hot spots on the surface of single early type stars proposed by the *RXTE* observations (Smith et al., 1998).

Secondly lets consider the binary systems. Some case of T-Tauri (possibly binaries) stars show a high temperature and a bright flare but still did not exceed 5 keV in temperature and did not reach to 10^{33} erg s^{-1} in luminosity (Koyama et at. 1994). Most are lower temperature and less luminous. The high mass binaries like GS0834-430 and Cep X-4, which contain an Be main star with a companion neutron star, are commonly observed as X-ray pulsars and show a power-law spectrum with a high energy cut and with strong low ionization 6.4 keV iron line. The mean of the iron line energies is 6.5 keV (Aoki et al., 1992, Koyama et al., 1991, Nagase 1997 references there in). The Cen X-3 show a weak iron line with 6.7 keV but 6.4 keV line pronounced to 6.7 keV (Nagase 1997). This is simply understood that strong stellar wind from main star accretes to a compact star and produces X-rays on the surface of a compact star and illuminate the cold wind and produce strong neutral iron line because of a large covering fraction to the accreting wind. The weak 6.7 keV iron line comes from possibly an accretion disk formed around the neutron star. However, the most case, the wind accretions do not form an accretion disk around the neutron star. The accretion onto a polar caps are common to make X-ray pulsars. This wind is cold enough to produce a strong 6.4 keV neutral iron line. This conflicts to the strong 6.7 and 6.9 keV highly ionized lines of γ Cas system. In case of low mass X-ray binaries like MXB1636-36, the spectrum can be best explained by a modified blackbody (or sum of multi-temperature blackbodies) with a characteristic temperature of 1 to 2 keV and a very weak iron line at 6.7 keV (Mitsuda et al. 1984). This line originates from the irradiated surface of the accretion disk but the covering factor is very low resulting a weak iron line. Recentry Asai et al. pointed out that an extremely low luminosity case of X 1608-522 showed a thermal spectrum which can be fitted by TB of 1 keV but almost no iron lines (Asai et al., 1996). These types of spectrum are also inconsistent with the thin thermal spectrum with the highly ionized strong iron lines of γ Cas .

Based on the known X-ray emitters above, the high temperature of 10 keV and the highly ionized iron line at 6.7 and 6.9 keV which are consistent to the temperature, are fully consistent with the known white dwarf X-ray system. The high temperature of 10 keV are common to the system (Mukai and Shiokawa 1993) and the three set of iron lines are also common to the white dwarf system (Fujimoto and Ishida 1997, Done et al. 1997, Ishida et al. 1997, Kallman et al. 1996). The requirement of a low temperature component of Ne line is also observed from some white dwarf system (Nousek et al.1994, Ishida et al. 1994). Probably, no pulsation of X-ray suggests an accreting non-magnetic white dwarf.

The only difficulty known to this idea is the low expected X-ray luminosity because of a large separation required from the no known orbital motion more than 10 km s^{-1} for γ Cas (Cowley et al. 1976, Parmar et a.1993). This strongly limits the binary separation between two stars. If we use the mass of the main star as $16M_{\odot}$, we can set the lower limit of the binary separation should be more than $300R_{\odot}\sin i$ (Cowley et al. 1976). This large separation required a low luminosity of the system. This conflicts the moderately luminous γ Cas . So, we have recalculated a probable luminosity of X-rays luminosity from this system based on the most recent observational wind parameters around the Be star γ Cas (Stee et al. 1995). We simply assume accretions of wind materials captured within the accretion radius as a function of orbital separation and wind parameters. Figure 4 shows the results of this calculation. Within the wind parameters, the observed luminosity of 10^{33} erg s^{-1} can be explained, if the orbital separation is less than $300R_{\odot}$ and this corresponds to 5 km s^{-1} in orbital motion and 150 days in orbital period for γ Cas . These orbital velocity and period will not be observable in the present observations and consistent with no observable orbital motion. The most recent measurement of the distance to γ Cas by Hipparcos of 190 pc reduces the required luminosity and supports our results (Perryman et al., 1997, ESA SP-1200).

In summary, the *ASCA* spectrum of γ Cas , 10 keV in temperature and three iron lines are naturally and simply explained by a white dwarf binary model. The lack of luminosity mentioned before in the previous papers are reconsidered based on the most recent wind parameters and we found that the wind of γ Cas can supply enough luminosity satisfying the observed value and this can be achieved within no observed orbital motion in this system.

The authors would like to express their thanks to Ezuka at ISAS for his assistances in analyzing the data at early stage. We also thank M. Smith for his kind discussions with us. TM was supported in part by the Grant-in Aid for Science Research by the Ministry of Education, Science, Sports and Culture.

References

Asai K., Dotani T., Mitsuda K., Hoshi R., Vaughan B., Tanaka Y., Inoue H. 1996, PASJ 48, 257

Chlebowski T., Harnden F.R. Jr. 1989, ApJ 341, 427

Corcoran M.F., Waldron W.L., MacFarlane J.J., Chen W., Pollock A.M.T., Torii K., Kitamoto S., Miura N., Egoshi M., Ohno Y. 1994, ApJ 436, L95

Cowley A.P., Rogers L., Hutchings J.B. 1976, PASP 88, 911

Done C., Osborne J.P. 1997, MNRAS 288, 649

Frontera F., Dal Fiume D., Robba N.R., Manzo G., Re S., Costa E. 1987, ApJ 320, L127

Fujimoto R., Ishida M. 1997, ApJ 474, 774

Haberl F. 1995, A&A 296, 685

Hoffleit D., Warren W.H. Jr. 1991, *The Bright Star Catalogue, 5th Revised Ed.* (Astronomical Data Center)

Horaguchi T., Kogure T., Hirata R., Kawai N., Matsuoka M., Murakami T., Doazan V., Slettebak A., Huang C.C., Cao H., Guo Z., Huang L., Tsujita J., Ohshima O., Ito Y. 1994, PASJ 46, 9

Ishida et al. 1994, PASJ 46, L81

Ishida M., Matsuzaki K., Fujimoto R., Mukai K., Osborne J.P. 1997, MNRAS 287, 651

Kallman T.R., Mukai K., Schlegel E.M., Paerels F.B. 1996, ApJ 466, 973

Koyama K., Maeda Y., Tsuru T., Nagase F., Skinner S. 1994, PASJ 46, L93

Makishima, K. et al., 1996, PASJ, 171

Marlborough J.M., Snow T.P. Jr., Slettebak, A. 1978, ApJ 224, 157

Mason K.O., White N.E., Sanford P.W. 1976, Nature 260, 690

Mitsuda K., Inoue H., Koyama K., Makishima K., Matsuoka M., Ogawara Y., Shibazaki N., Suzuki K., Tanaka Y., Hirano T. 1984, PASJ 36, 741

Murakami T., Koyama K., Inoue H., Agrawal P.C. 1986, ApJ 310, L31

Nagase F., Zylstra G., Sonobe T., Kotani T., Inoue H., Woo J. 1997, ApJ 436, L1

Nousek et al. 1994, ApJL 436, L19

Parmar, A.N., Israel, G. L., Stella, L., White, N., 1993, A&A, 275, 227

Perryman M.A.C., Lindegren L., Kovalevsky J., Høg E., Bastian U., Bernacca P.L., Crézé M., Donati F., Grenon M., Grewing M., van Leeuwen F., van der Marel H., Mignard F., Murray C.A., Le Poole R.S., Schrijver H., Turon C., Arenou F., Froeschlé M., Petersen C.S. 1997, A&A 323, L49

Rappaport S., van den Heuvel E.P.J. 1982, in *Be STARS*, ed. Jaschek M., Groth H.-G. (IAU), p.327

Schmidt-Kaler T. 1964, Astr. Inst. Univ. Bonn, 70

Serlmitsos, P.J., et al., 1995, PASJ, 105

Smith M., et al. 1998, ApJ submitted

Stee Ph., de Araújo F.X., Vakili F., Mourard D., Arnold L., Bonneau D., Morand F., Tallon-Bosc I. 1995, A&A 300, 219

White N.E., Swank J.H., Holt S.S., Parmar A.N. 1982, ApJ 263, 277

Yamashita, A., T. Dotani, M. Bautz, G. Crew, H. Ezuka, K. Gendreau, T. Kotani, K. Mitsuda, C. Otani, A. Rasmussen, G. Ricker, H. Tsunemi, 1997, IEEE, NS-44, 847

Table 1.. **Fitting parameters of the spectrum** *

Model	Power-law + Gaussian	Raymond-Smith	Raymond-Smith + Gaussian (6.4keV + Ne)
Photon index	1.59 ±0.02		
Temperature (keV)		10.7 ±0.6	10.5 ±0.6
Abundance		0.35 ±0.08	0.33 ±0.08
Line Energy (keV)	$6.66\ ^{+0.10}_{-0.08}$		6.40 (frozen)
Sigma (keV)	0.1 ±0.1		< 1.3
Equivalent width (eV)	$187\ ^{+67}_{-73}$		$60\ ^{+253}_{-35}$
Hydrogen column density ($\times 10^{21}$ atoms cm^{-2})	2.05 ±0.09	1.53 ±0.07	1.54 ±0.07
χ^2 ‡	235.9 (246)	218.2 (248)	210.1 (246)
Model flux (0.5–10 keV) ($\times 10^{-12}$ ergs cm^{-2} s^{-1})	1.60	1.54	1.54
Model flux (2–10 keV) ($\times 10^{-12}$ ergs cm^{-2} s^{-1})	1.24	1.18	1.18

* All errors are ± 90% errors.
‡ In the parentheses are the degree of freedom.

Figure captions

Fig. 1a-1c
Light curves at three independent observations, which were started on 1996 January 18, March 3, and September 4 with a time resolution of 16 s in 2–10 keV. Each plot is summed over the four instruments on-board.

Fig. 1d
Close up view of the figure 1c at 25.53 hour with a time resolution of 4 s. Rapid time variability of 10 s is seen in this data. This limits the emission size.

Fig. 2.
A XRONOS power density spectrum for the avaraged data of figure 1a to 1c. There was no clear periodicity but 1/f type fluctuation is clear.

Fig. 3a-3c.
A spectrum averaged over the three data sets. (a) Power-law with a Gaussian line. (b) The simple R-S model as abundance and temperature are free. (c) The iron at 6.4 keV and Ne are artificially added beside the model of figure-3b. The best fit paprameters for each fit are listed in table-1.

Fig. 4a and 4b.
Estimated X-ray luminosity as a function of orbital separation together with an orbital velosity and an orbital period. If we use the most recent wind parameters of γ Cas , 10^{33} erg s^{-1} can be achievable at the orbital separation of less than $300 R_{\odot}$.

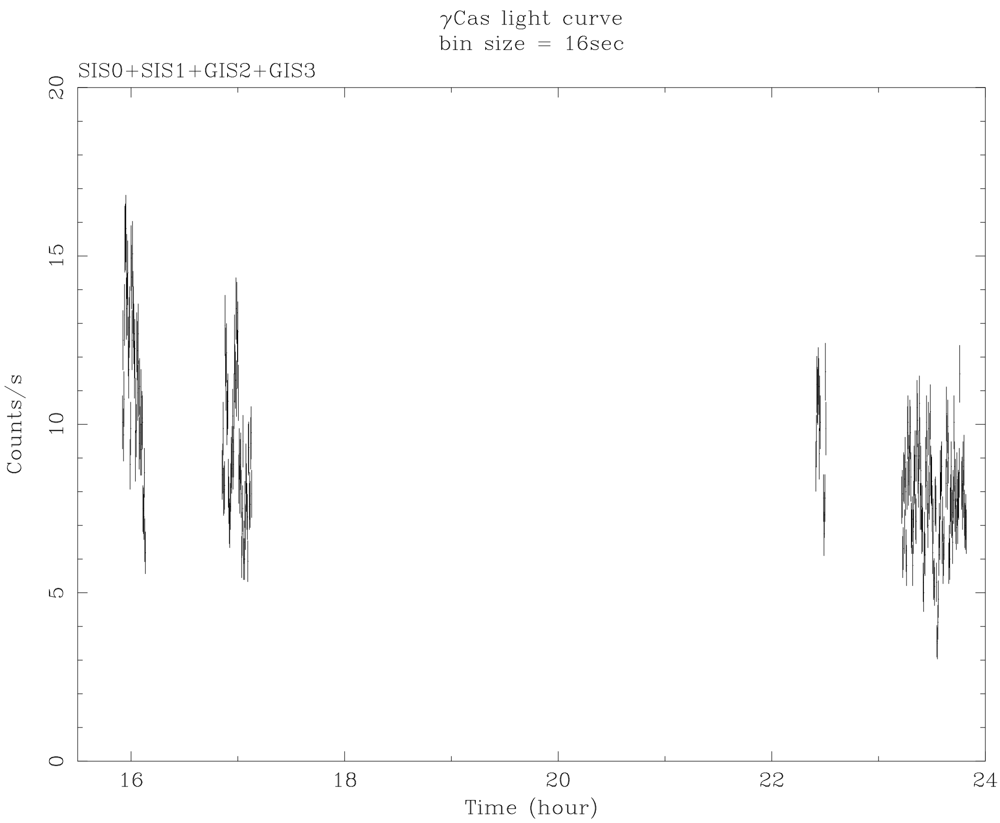
γCas light curve
bin size = 16sec
SIS0+SIS1+GIS2+GIS3
Counts/s
0
5
10
15
20
16
18
20
22
24
Time (hour)

Figure 1a :

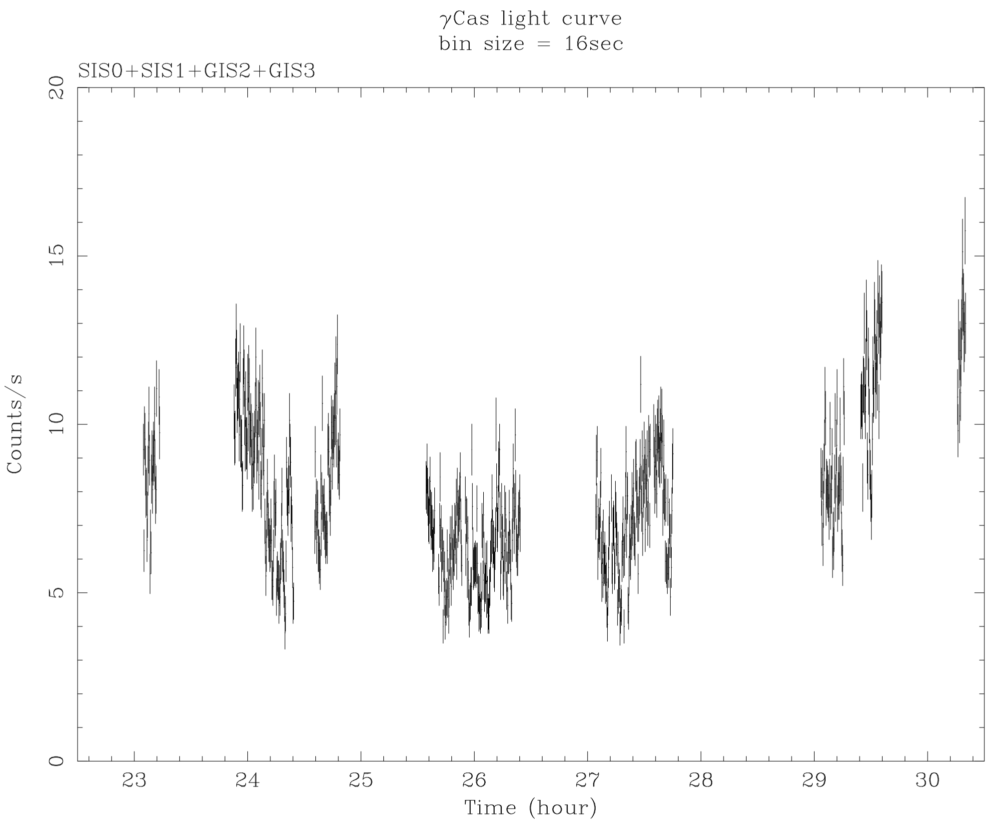
γCas light curve
bin size = 16sec
SIS0+SIS1+GIS2+GIS3
Counts/s
Time (hour)
0
5
10
15
20
23
24
25
26
27
28
29
30

Figure 1b :

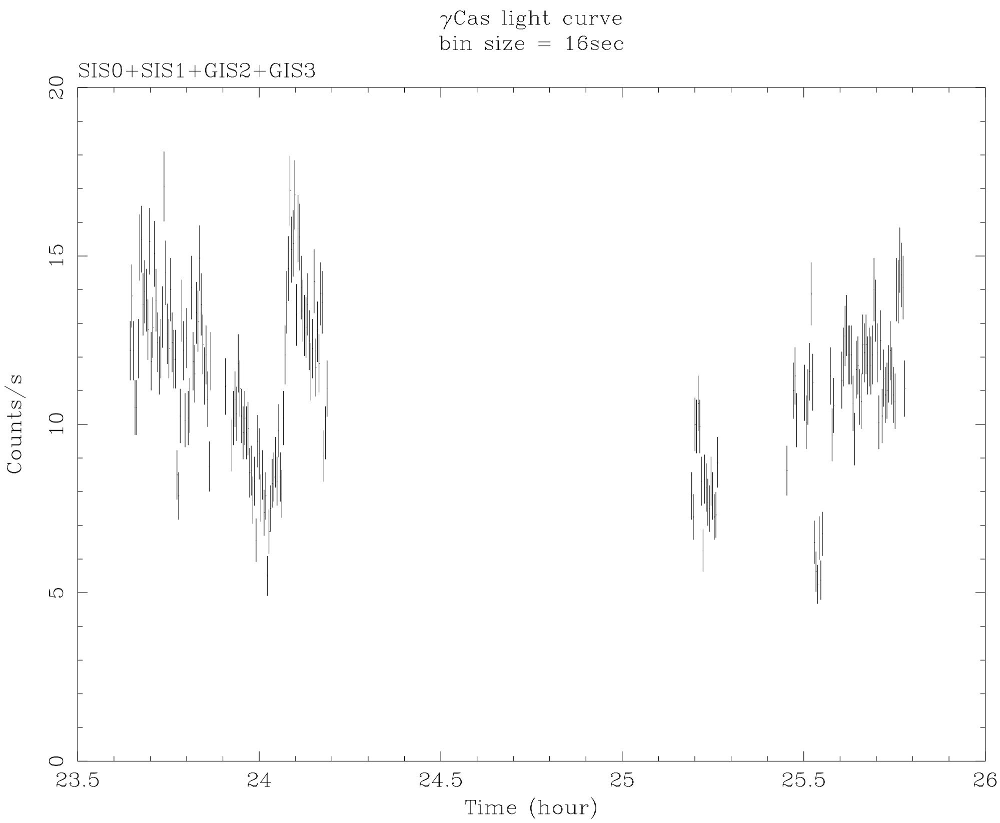
γCas light curve
bin size = 16sec
SIS0+SIS1+GIS2+GIS3
Counts/s
Time (hour)
0
5
10
15
20
23.5
24
24.5
25
25.5
26

Figure 1c :

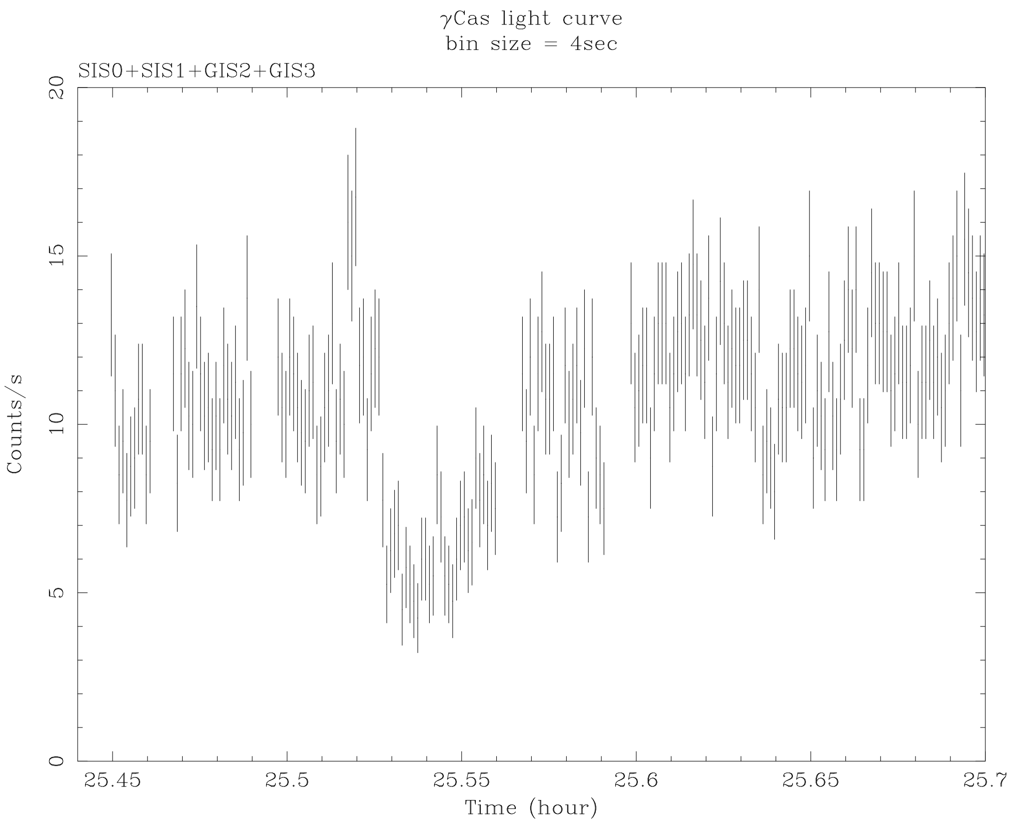
γCas light curve
bin size = 4sec
SIS0+SIS1+GIS2+GIS3
Counts/s
0
5
10
15
20
25.45
25.5
25.55
25.6
25.65
25.7
Time (hour)

Figure 1d :

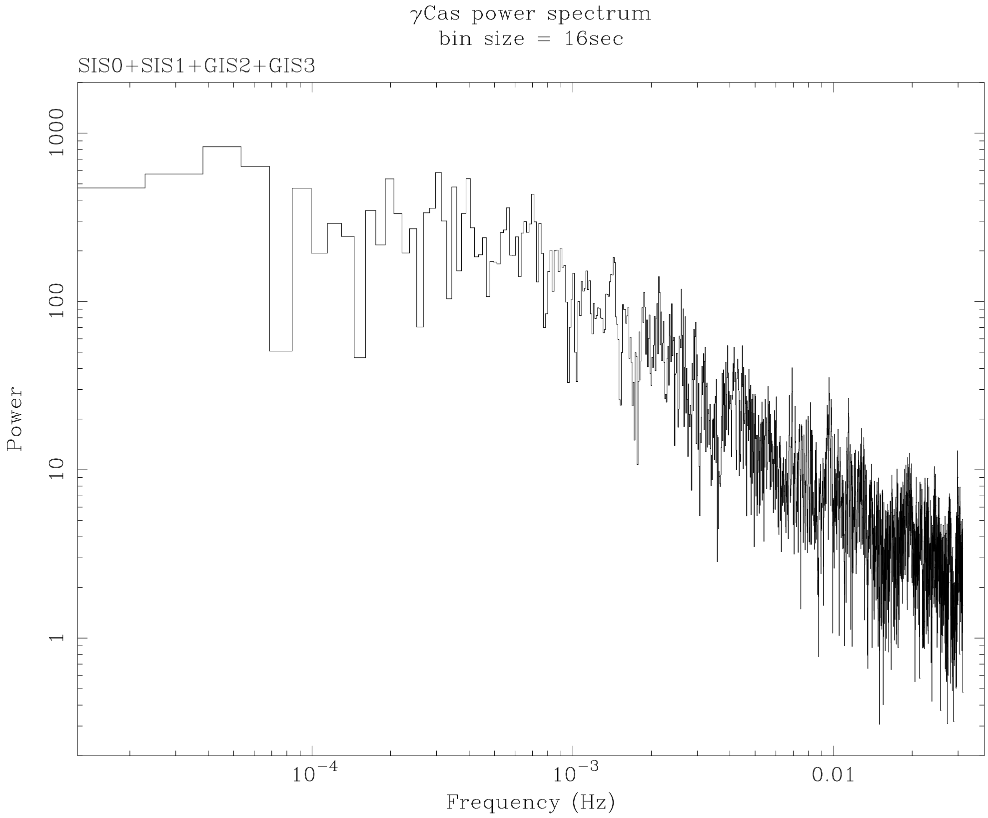
γCas power spectrum
bin size = 16sec
SIS0+SIS1+GIS2+GIS3
Power
1000
100
10
1
10^{-4}
10^{-3}
0.01
Frequency (Hz)

Figure 2 :

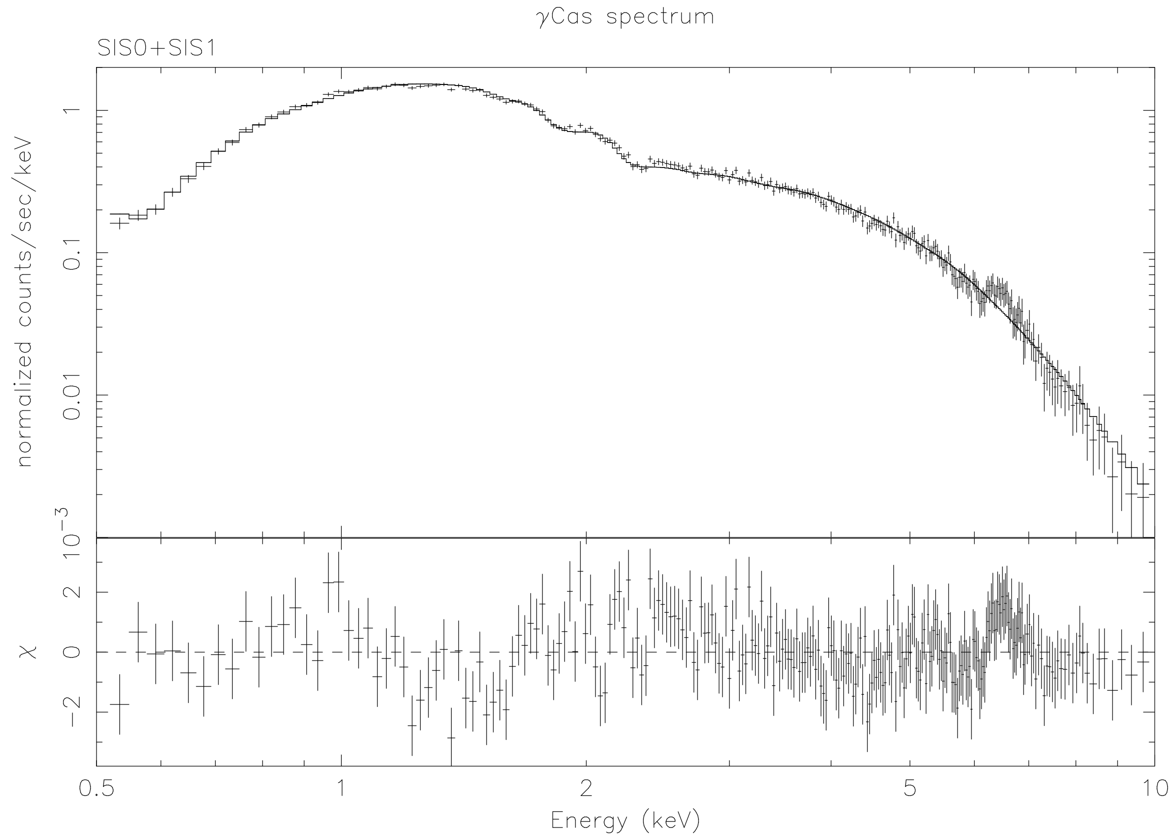
γCas spectrum
SIS0+SIS1
normalized counts/sec/keV
1
0.1
0.01
10^-3
χ
2
0
−2
0.5
1
2
5
10
Energy (keV)

Figure 3a :

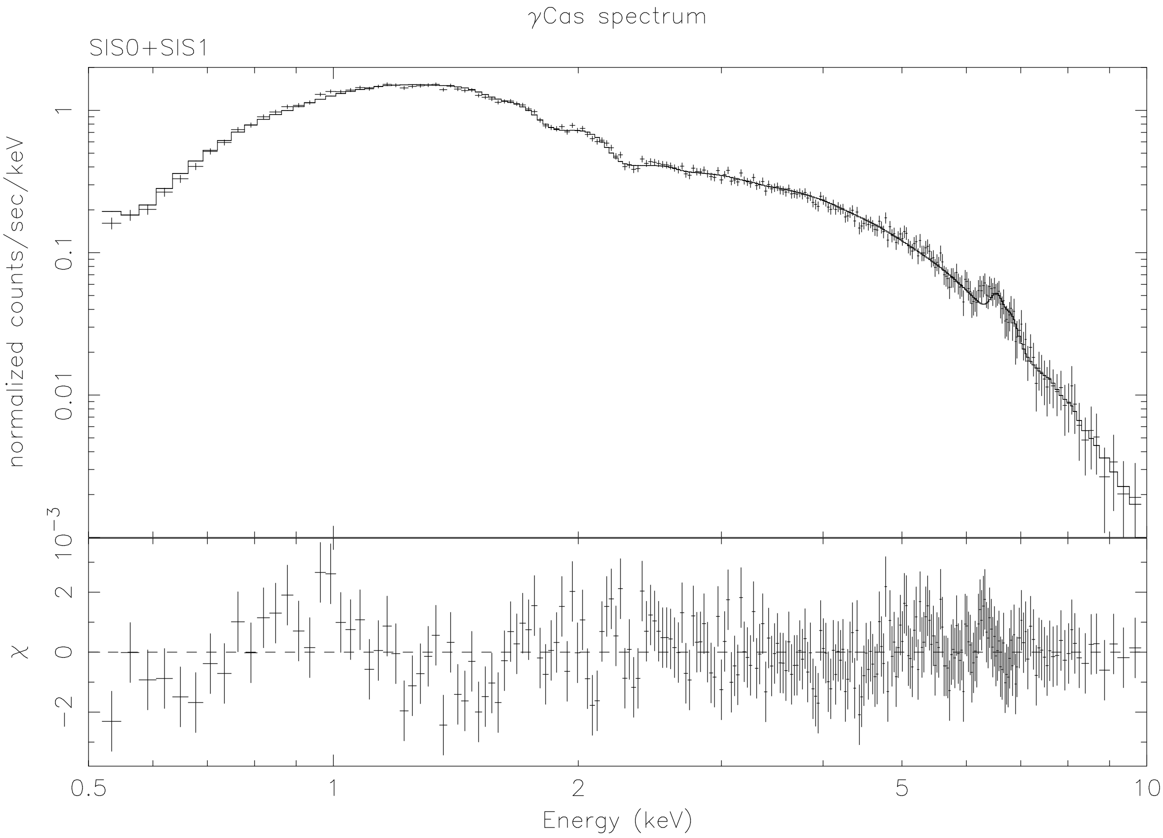
γCas spectrum
SIS0+SIS1
normalized counts/sec/keV
1
0.1
0.01
10⁻³
χ
2
0
−2
0.5
1
2
5
10
Energy (keV)

Figure 3b :

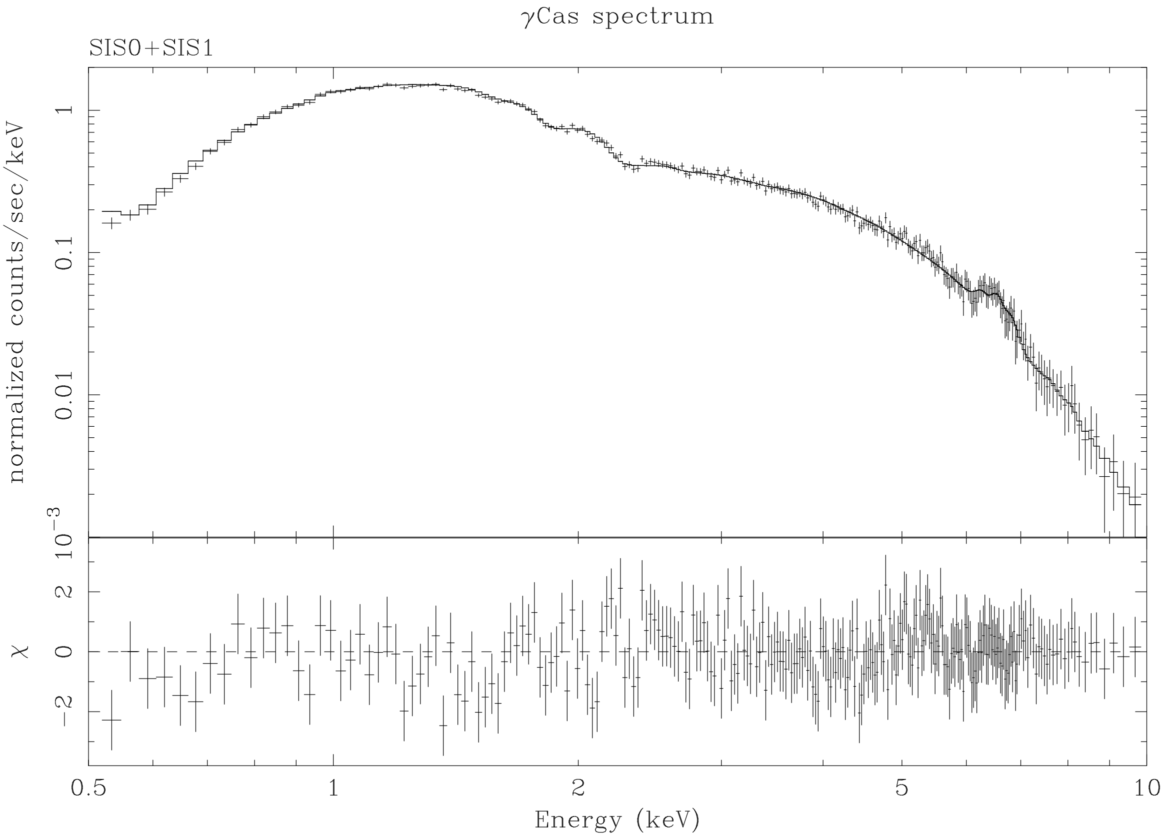
γCas spectrum
SIS0+SIS1
normalized counts/sec/keV
1
0.1
0.01
10⁻³
χ
2
0
−2
0.5
1
2
5
10
Energy (keV)

Figure 3c :

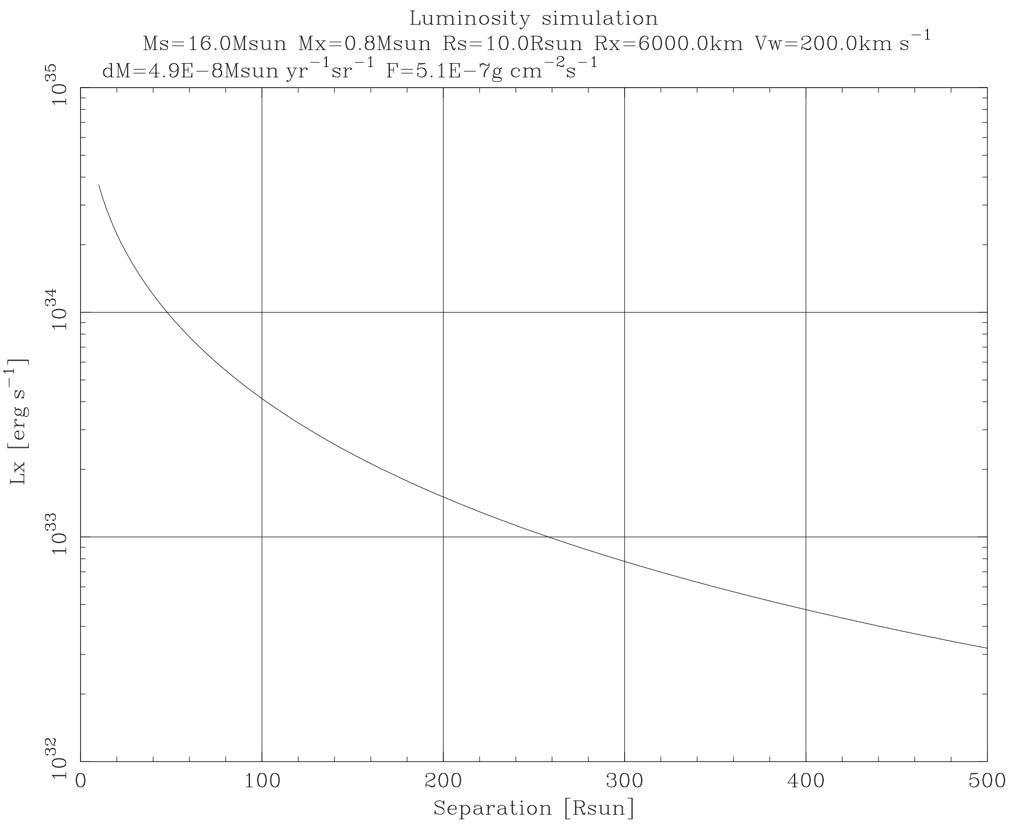

Figure 4a :

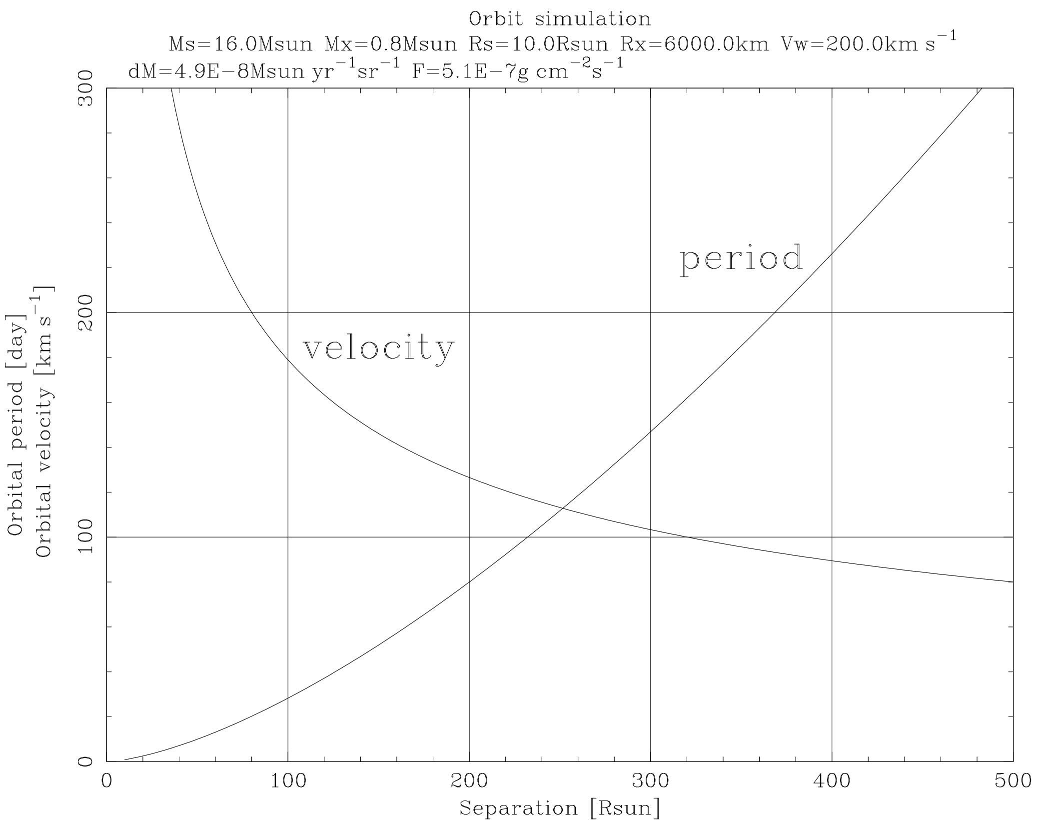

Figure 4b :